

# On the Investigations of Electron Density in the Solar Corona with VLBI

Dan Aksim, Alexey Melnikov, Dmitry Pavlov, Sergey Kurdubov

Institute of Applied Astronomy of the Russian Academy of Sciences

## Abstract

The Sun's corona has interested researchers for multiple reasons, including the search for solution for the famous coronal heating problem and a purely practical consideration of predicting geomagnetic storms on Earth. There exist numerous different theories regarding the solar corona; therefore, it is important to be able to perform comparative analysis and validation of those theories. One way that could help us move towards the answers to those problems is the search for observational methods that could obtain information about the physical properties of the solar corona and provide means for comparing different solar corona models.

In this work we present evidence that VLBI observations are, in certain conditions, sensitive to the electron density of the solar corona and are able to distinguish between different electron density models, which makes the technique of VLBI valuable for solar corona investigations. Recent works on the subject used a symmetric power-law model of the electron density in solar plasma; in this work, an improvement is proposed based on a 3D numerical model.

## Electron density models

Typically, when it comes to measuring the electron density in the solar corona by means of radio sounding, most works tend to adopt a simple symmetric power-law model of the electron density

$$N_e(r) = N_0/r^\alpha, \quad (1)$$

where  $N_0 = N_e(R_\odot)$  is an estimated parameter and  $\alpha$  is either estimated or set to be approximately equal to 2, which corresponds to electrons drifting away from the Sun with constant velocity. As follows from the continuity equation, the density should fall faster than  $1/r^2$  if the electrons are accelerating and slower if they are decelerating.

Values of  $N_0$  and  $\alpha$  vary between different works, which is usually contributed to variances in solar activity. They vary even between different sides of the Sun during a single experiment with a single spacecraft, which raises concern about the validity of symmetric models.

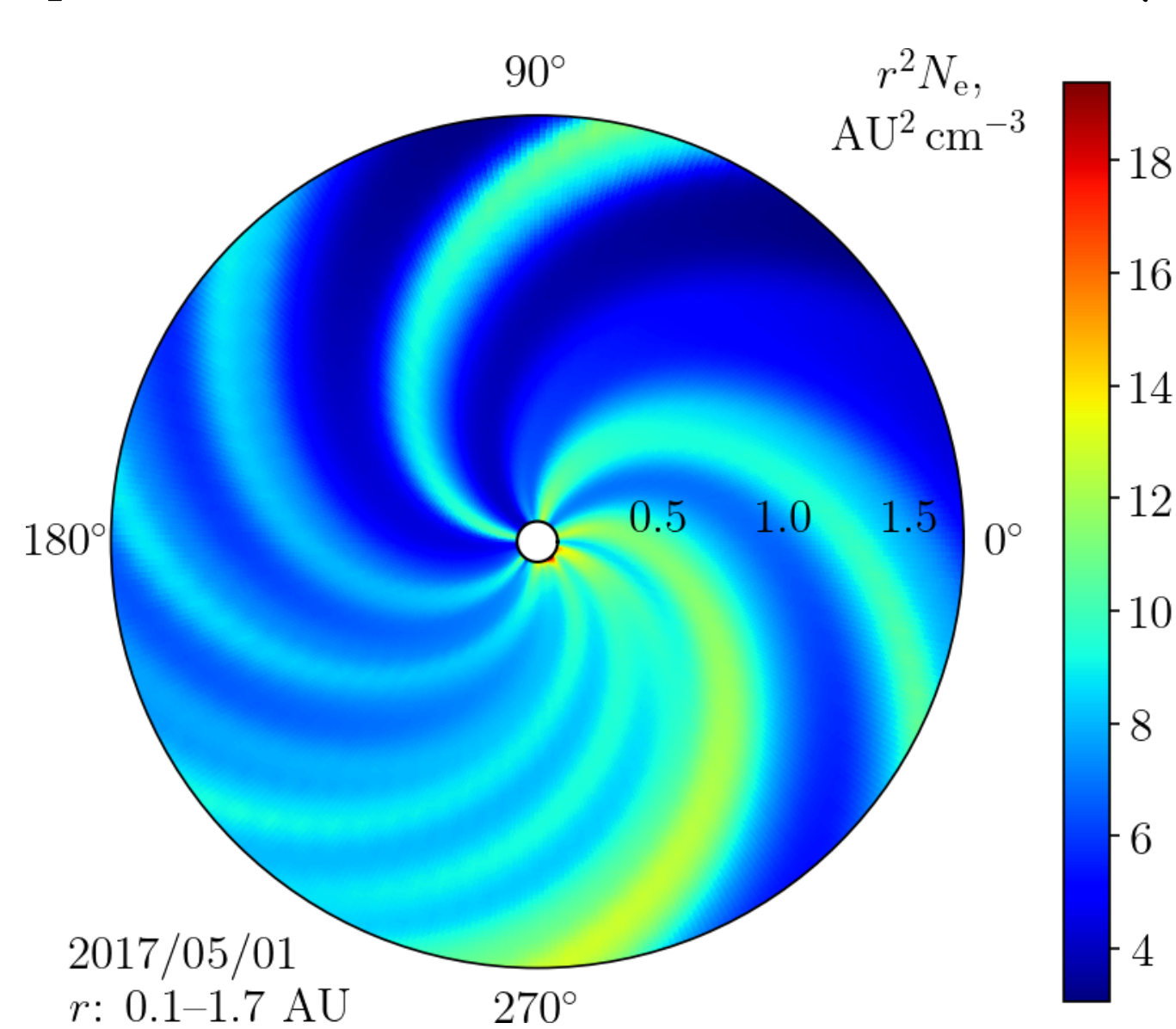


Figure 1: Solar wind electron density from the ENLIL model (in  $0^\circ$  latitude plane in HEEQ coordinate system)

Simulation data for ENLIL and AWSoM models is provided by request on the CCMC website (<http://ccmc.gsfc.nasa.gov/>).

## Radio wave propagation in the corona

The group refractive index in plasma is

$$n_{gr}(r, f) \approx 1 + \frac{N_e(r)}{2N_{crit}(f)}, \quad (2)$$

where  $N_e$  is the electron density and  $N_{crit}(f) = 4\pi^2 \epsilon_0 m_e f^2 / e^2$  is the critical density at frequency  $f$ . Neglecting the light path curvature and taking an integral along a straight line, dispersive time delay in the solar corona between points  $\mathbf{r}_a$  and  $\mathbf{r}_b$  is

$$\tau_{cor} = \int_{r_a}^{r_b} (n_{gr}(s, f) - 1) ds \approx \frac{1}{2N_{crit}(f)} \left[ \int_p^{r_a} \frac{N_e(r) r dr}{\sqrt{r^2 - p^2}} + \int_p^{r_b} \frac{N_e(r) r dr}{\sqrt{r^2 - p^2}} \right], \quad (3)$$

where  $r_a = |\mathbf{r}_a|$  and  $r_b = |\mathbf{r}_b|$ , and  $p$  is the impact parameter, i.e. the distance of closest approach of the light ray to the Sun.

## VLBI data analysis

If the delays measured by VLBI at S and X band frequencies  $f_s$  and  $f_x$  are  $\tau_s$  and  $\tau_x$ , then the dispersive contribution to  $\tau_x$  consists of delays in the corona, the ionosphere, and in the receiver hardware, and is written as

$$\Delta\tau_{disp,x} = \frac{f_s^2}{f_x^2 - f_s^2} (\tau_x - \tau_s) = \Delta\tau_{cor} + \Delta\tau_{ion} + \Delta\tau_{inst}. \quad (4)$$

In this work, the ionospheric delay  $\Delta\tau_{ion}$  was computed from global ionosphere maps (GIMs), which are constructed from GPS satellite data. To avoid correlations between the solar corona parameter and instrumental biases, we divide observations into two groups: the first group with elongations above  $15^\circ$  and the second—with elongations below  $15^\circ$ . The first group is used to find  $\Delta\tau_{inst}$ , the second group—to find the electron density multiplier  $N_0$ .

## Results

All VLBI sessions that have been previously used in other works for solar corona parameters estimation are 12 research and development (R&D) sessions that took place in 2011–2012 and sessions AUA020 and AOV022 from 2017 and 2018.

Table 1: List of VLBI sessions

| Session | Date     | No. of obs. ( $< 15^\circ$ /Total) | Min. elong. | $N_{cm}^\dagger$ |
|---------|----------|------------------------------------|-------------|------------------|
| RD1106  | 11/11/29 | 33/3695                            | $4.0^\circ$ | 11               |
| RD1205  | 12/07/10 | 187/2953                           | $6.0^\circ$ | 34               |
| RD1206  | 12/08/28 | 193/1558                           | $3.8^\circ$ | 60               |
| RD1208  | 12/10/02 | 103/1918                           | $3.9^\circ$ | 15               |
| RD1209  | 12/11/27 | 57/2731                            | $4.3^\circ$ | 22               |
| RD1210  | 12/11/11 | 80/3540                            | $4.8^\circ$ | 12               |
| AUA020  | 17/05/01 | 1029/4010                          | $1.2^\circ$ | 945              |
| AOV022  | 18/05/01 | 3429/14099                         | $1.3^\circ$ | 3261             |

$^\dagger N_{cm}$  is no. of obs. with  $> 1$  cm diff. delay with model (1),  $N_0 = 10^{12} \text{ m}^{-3}$ ,  $\alpha = 2$ . It is a measure of the session's sensitivity to the corona.

Sessions used in this work are listed in Table 1. Out of 12 R&D sessions we picked 6 most sensitive to the solar corona by requiring that  $N_{cm} > 10$ . Observational geometry of the AUA020 session is shown in Figure 2. Session AOV022 was held precisely one year later, and thus its geometry is quite similar.

Solutions with the power-law model (1) were acquired for all sessions. During sessions RD1206, RD1208, and RD1209, strong coronal mass ejections (CMEs) happened, which made it impossible to apply the AWSoM data to these sessions. Because of that, solutions with the AWSoM model were obtained for all sessions except RD1206, RD1208, and RD1209.

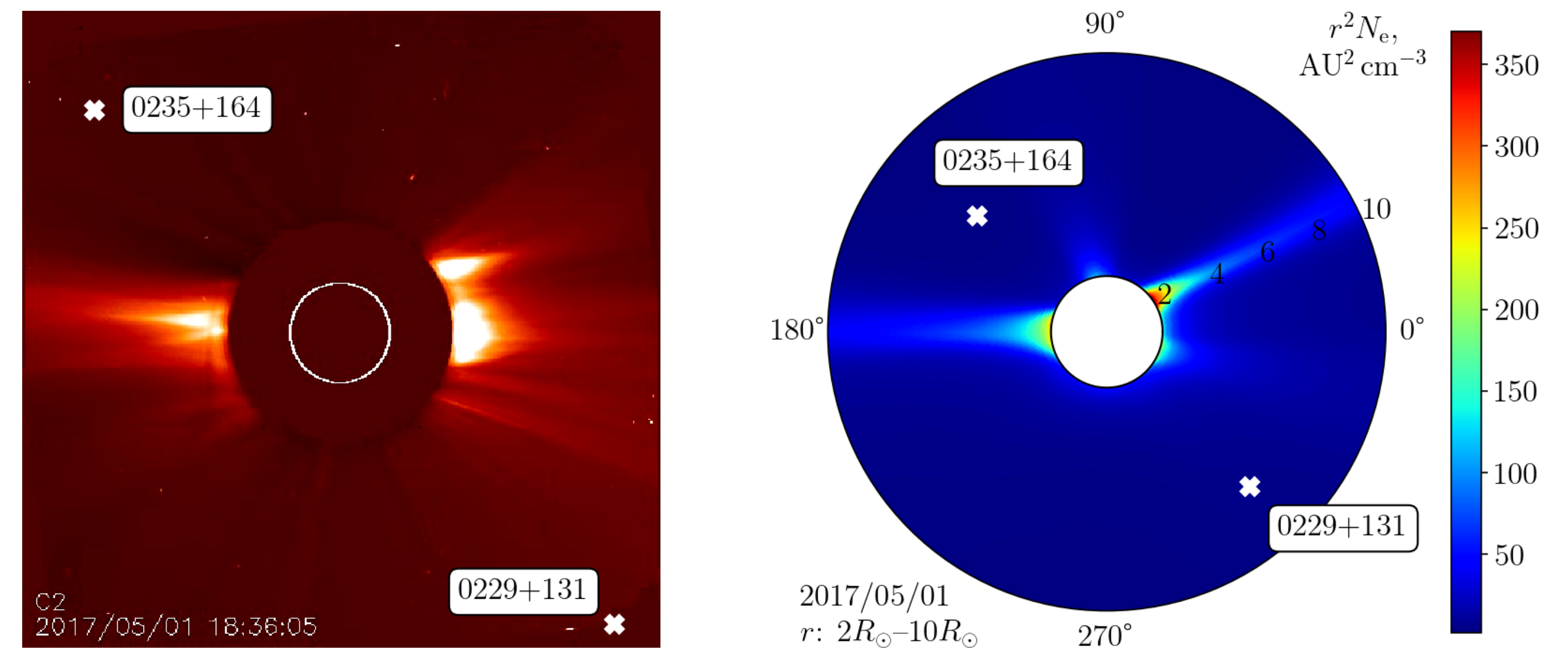


Figure 2: Observational geometry of the AUA020 session (as visible from Earth). LASCO C2 coronagraph image (left) and the solar corona electron density from the AWSoM model (right).

In the case of the AWSoM model, the estimated parameter was the unitless multiplier  $A$  of the electron density map. The model was run with default parameters, which, as the authors have noted, need further calibration and are not guaranteed to be the best. Thus, the multiplier  $A$  was artificially introduced to compensate, to some extent, for the uncertainties of the model input parameters. Values of  $N_0$  and  $A$  and their  $1\sigma$  uncertainties for each session are given in table 2.

Table 2: Estimated values

| Session | Outliers | $\alpha$ | Soja et al. <sup>†</sup>       | Power law <sup>††</sup>        |         | AWSoM            |         |
|---------|----------|----------|--------------------------------|--------------------------------|---------|------------------|---------|
|         |          |          | $N_0 (10^{12} \text{ m}^{-3})$ | $N_0 (10^{12} \text{ m}^{-3})$ | RMS (m) | $A$              | RMS (m) |
| RD1106  | 114      | 2        | $0.0 \pm 0.4$                  | $0.10 \pm 0.47$                | 0.0485  | $-1.43 \pm 1.28$ | 0.0476  |
| RD1205  | 214      | 2        | $0.5 \pm 0.3$                  | $1.08 \pm 0.21$                | 0.0211  | $0.21 \pm 0.12$  | 0.0223  |
| RD1206  | 98       | 2        | $0.3 \pm 0.1$                  | $0.34 \pm 0.15$                | 0.0288  | —                | —       |
| RD1208  | 56       | 2        | $1.5 \pm 0.4$                  | $0.86 \pm 0.20$                | 0.0315  | —                | —       |
| RD1209  | 234      | 2        | $0.1 \pm 0.3$                  | $0.48 \pm 0.25$                | 0.0497  | —                | —       |
| RD1210  | 51       | 2        | $2.5 \pm 0.6$                  | $0.00 \pm 0.68$                | 0.0482  | $0.93 \pm 0.80$  | 0.0478  |
| AUA020  | 155      | 2.2      | $0.61 \pm 0.05$                | $0.57 \pm 0.01$                | 0.0655  | $0.96 \pm 0.02$  | 0.0612  |
| AOV022  | 1203     | 2        | $0.44 \pm 0.005$               | $0.43 \pm 0.02$                | 0.15607 | $0.84 \pm 0.04$  | 0.1530  |
|         |          | 2.3      | —                              | $0.60 \pm 0.03$                | 0.15604 | —                | —       |

<sup>†</sup> Values were taken from [2] for R&D sessions, from [3] for AUA020, and from [4] for AOV022.

The values of  $N_0$  in Table 2 generally agree within the uncertainty with the ones provided in [2, 3, 4], and agreement is almost perfect for AUA020 and, in case of  $\alpha = 2$ , AOV022. The only session with considerable difference in solutions is RD1210, where Soja's result is  $2.5 \pm 0.6$  and ours is  $0.00 \pm 0.68$ . In fact, taking the uncertainty into account, even these results agree within  $3\sigma$ .

Although least-squares estimations have succeeded at finding solutions for  $N_0$  and confirming the results obtained independently in [2, 3, 4], still, there is no evidence that the R&D sessions are sensitive to the choice of the solar corona model and to the parameters of the chosen model. Not only the  $N_0$  uncertainties for the R&D sessions are somewhat large, but, as shown in Figure 3, the post-fit residuals barely depend on the choice of the power  $\alpha$ , varying by less than 0.5–1 mm with  $\alpha$  changing from 1.4 to 2.5 and not even reaching minimum values for any given  $\alpha$ . Hence, from the perspective of the R&D sessions data, all possible power laws fit the electron density equally well, including those with extreme  $\alpha$  values that never occur in previously published papers and therefore seem unlikely in general. Furthermore, the residuals for the R&D sessions with the AWSoM model (given in Table 2) differ only slightly from those for the power law and fail to show any consistent relationship to them.

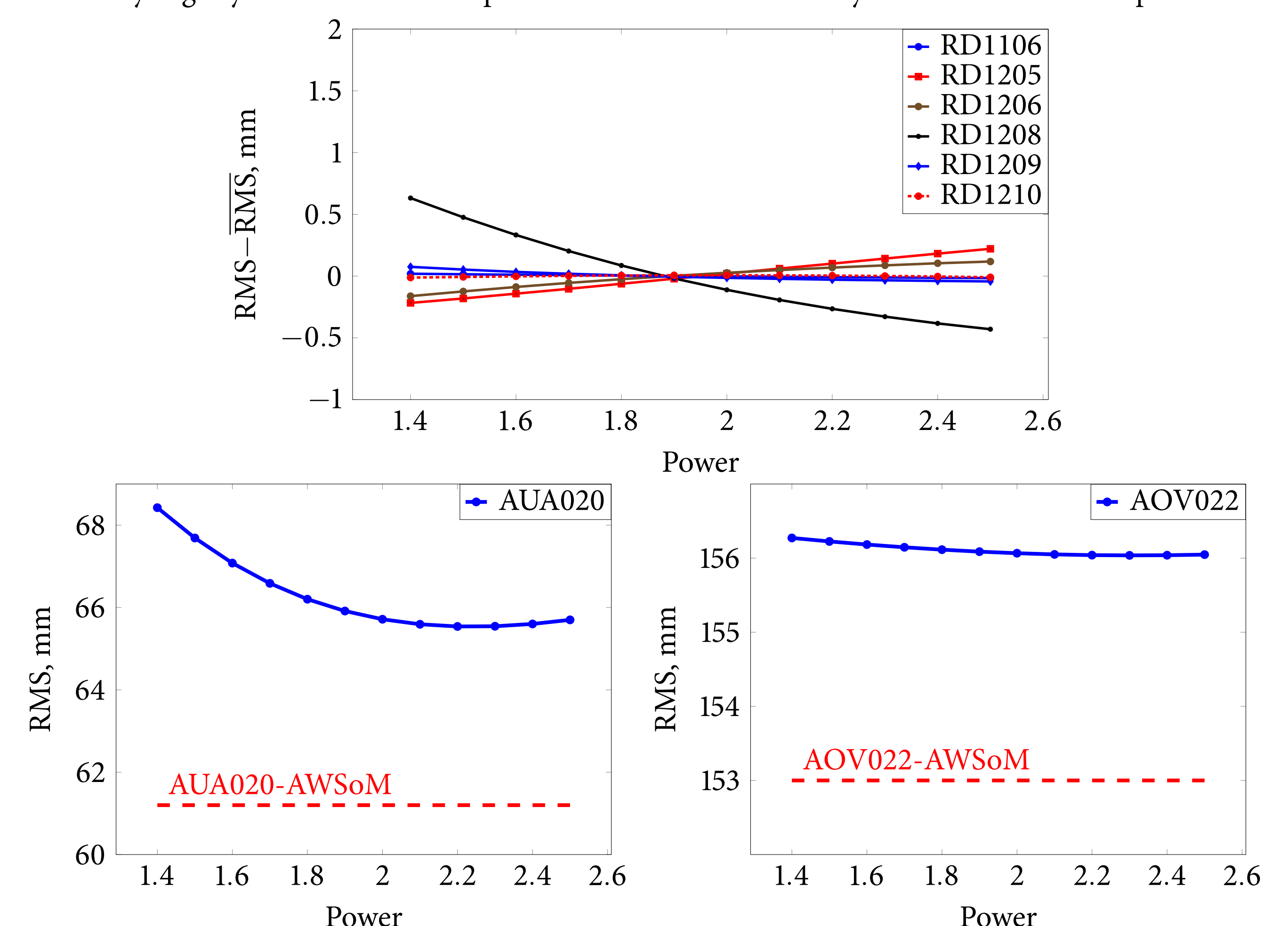


Figure 3: Dependencies of RMS errors on  $\alpha$ . For each  $\alpha$  the value of  $N_0$  is optimal, i.e. acquired via least squares.

## Conclusions

- VLBI is sensitive enough to the solar corona electron density to distinguish between different models and to allow for estimation of model parameters.
- We confirm previous results [2, 3, 4] and also note that the AUA020 and AOV022 sessions show superiority of the AWSoM model over the power law. We therefore suggest that the power law is not an accurate representation of the solar corona electron density and that further analysis can benefit from more sophisticated modern 3D solar corona models.
- To fully explore the possibilities that VLBI provides for comparing different solar corona models, we need more observational data, preferably of the likes of AUA020 and AOV022 in terms of the number of observations made close to the Sun and minimum elongation angles.

- [1] B. van der Holst et al. Alfvén wave solar model (AWSoM): Coronal heating. *The Astrophysical Journal*, 782, 2014.
- [2] B. Soja et al. Probing the solar corona with very long baseline interferometry. *Nature Communications*, 5(1), June 2014.
- [3] B. Soja et al. Solar corona electron density models from recent VLBI experiments AUA020 and AUA029, 2018.
- [4] B. Soja et al. Very long baseline interferometry as a tool to probe the solar corona, 2019.